Supporting Information for:

Main-chain/Side-chain type Phosphine Oxide-Containing Reactive Polymers Derived from same Monomer: Controllable RAFT Polymerisation and ring-opening Polycondensation

Jian Sun[a], Yu-Lin Hong[a], Chang Wang[a], Zhi-Wei Tan[a,c], Cheng-Mei Liu[a†]

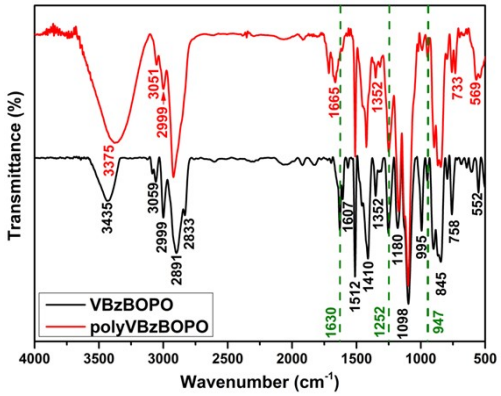

Figure S1. FT-IR spectra of VBzBOPO (black) and polyVBzBOPO (red).

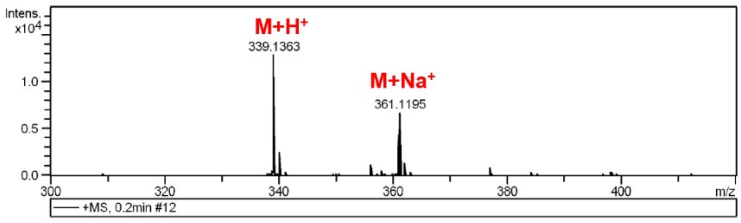

Figure S2. Mass spectrum of monomer VBzBOPO.

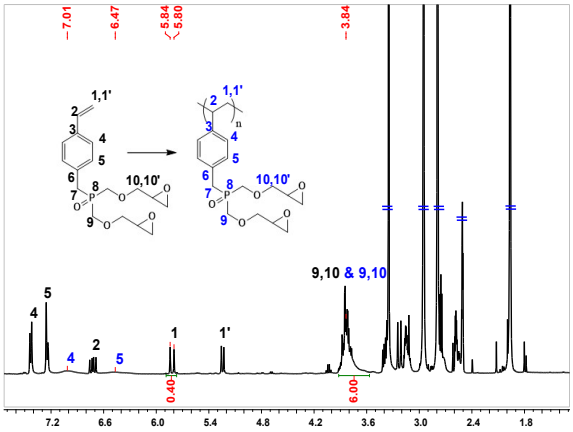

Figure S3. ^{1}H NMR spectrum of polymerization mixture (P1-1) in DMSO-d_6.

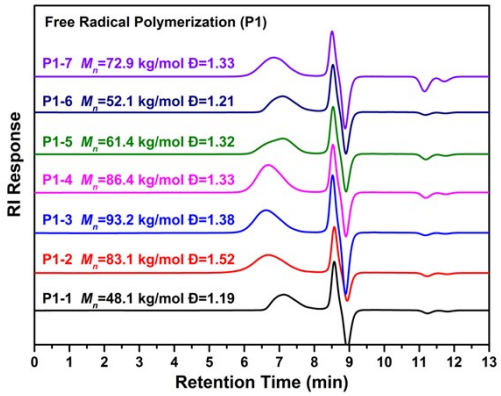

Figure S4. SEC elution curves of polyVBzBOPO (P1) synthesized by free radical polymerization.

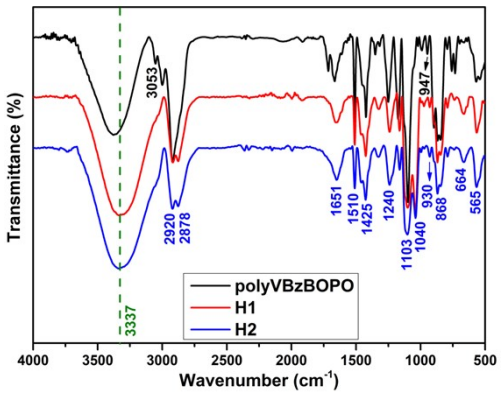

Figure S5. FT-IR spectra of polyVBzBOPO before and after hydrolysis reaction (H1 and H2).

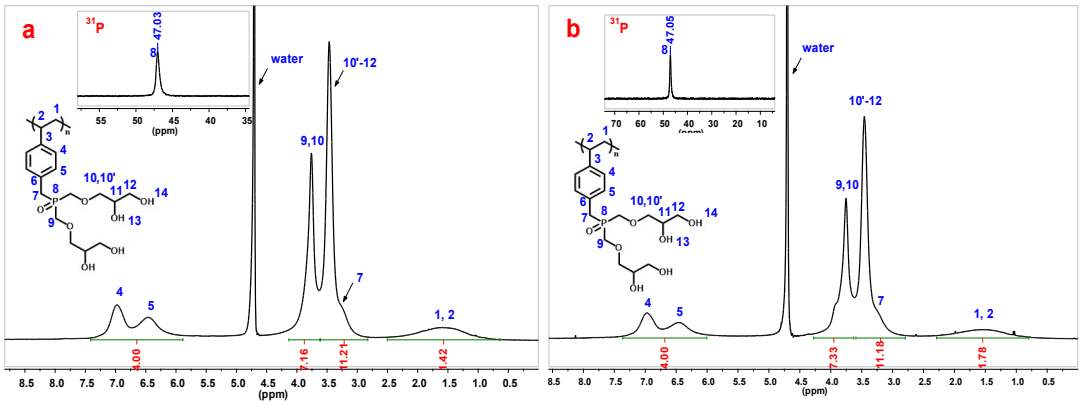

Figure S6. ^{1}H and ^{31}P (insert) NMR spectra of H1 (a) and H2 (b) in D_2O.

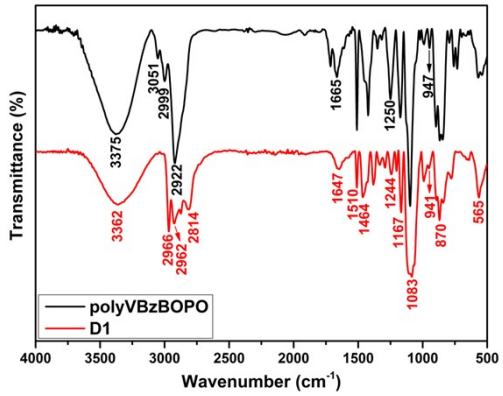

Figure S7. FT-IR spectra of polyVBzBOPO before and after post-polymerization modification with DEA (D1).

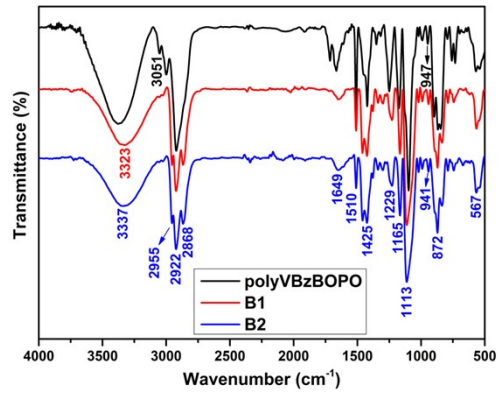

Figure S8. FT-IR spectra of polyVBzBOPO before and after post-polymerization modification with n-butanethiol (B1 and B2).

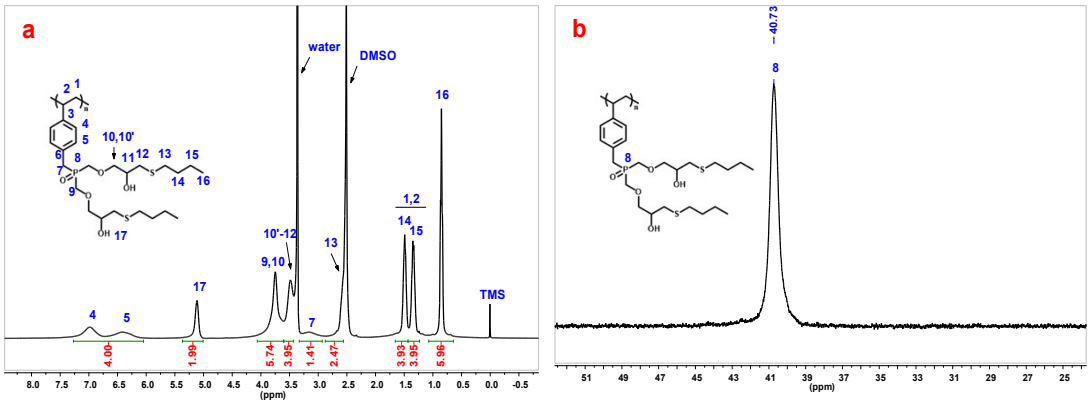

Figure S9. (a) ^{1}H and (b) ^{31}P NMR spectra of B2 in DMSO-d_6.

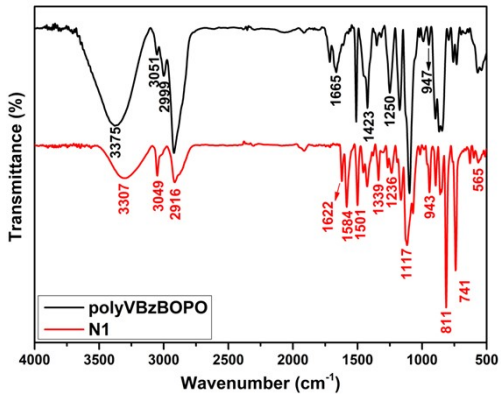

Figure S10. FT-IR spectra of polyVBzBOPO before and after post-polymerization modification with methyl 3-mercaptopropionate (N1).

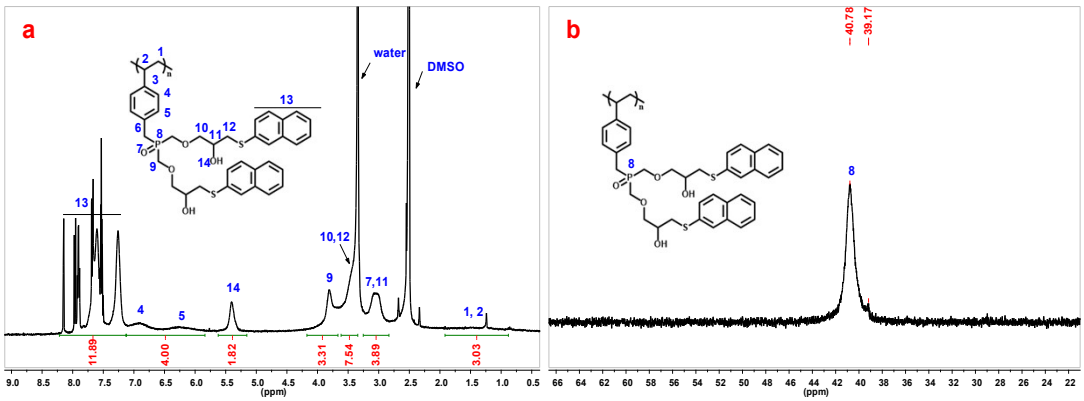

Figure S11. (a) ^{1}H and (b) ^{31}P NMR spectra of N1 in DMSO-d_6.

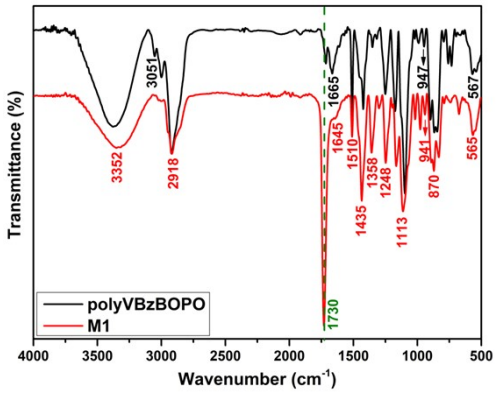

Figure S12. FT-IR spectra of polyVBzBOPO before and after post-polymerization modification with methyl 3-mercaptopropionate (M1).

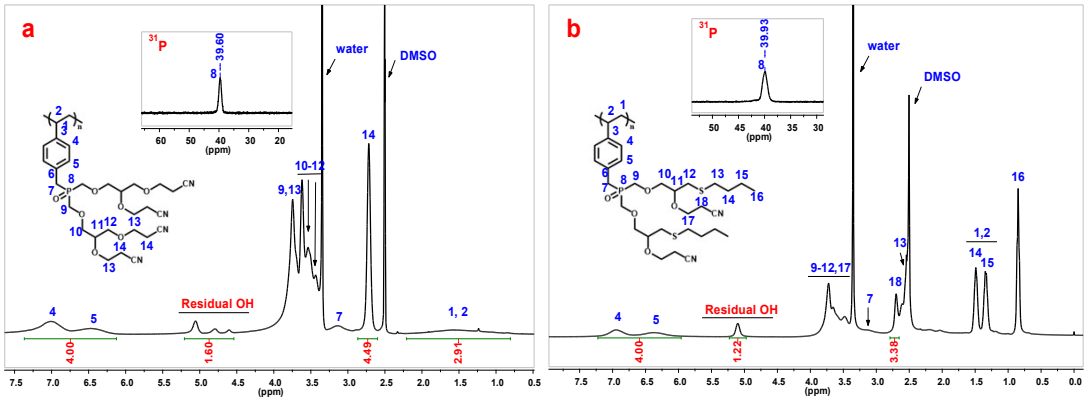

Figure S13. ^{1}H and ^{31}P (insert) NMR spectra of HAN (a) and BAN (b) in DMSO-d_6.

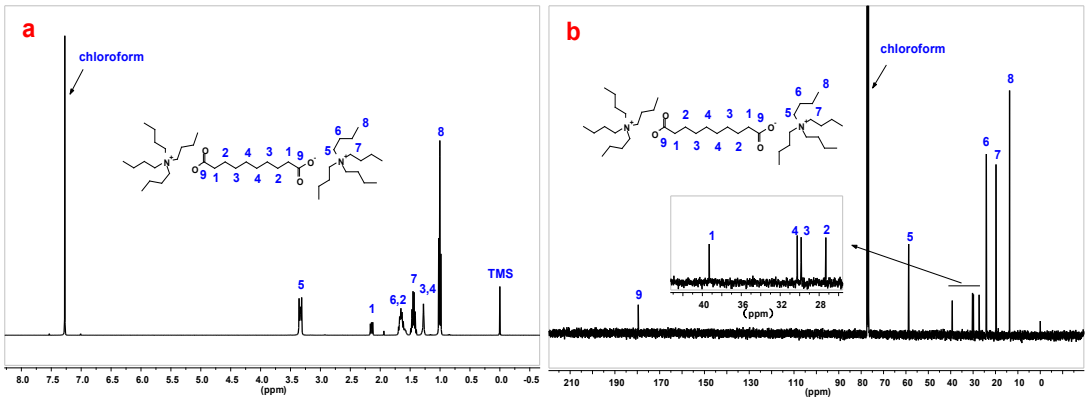

Figure S14. (a) ^{1}H and (b) ^{13}C NMR spectra of TBAS in $CDCl_3$.

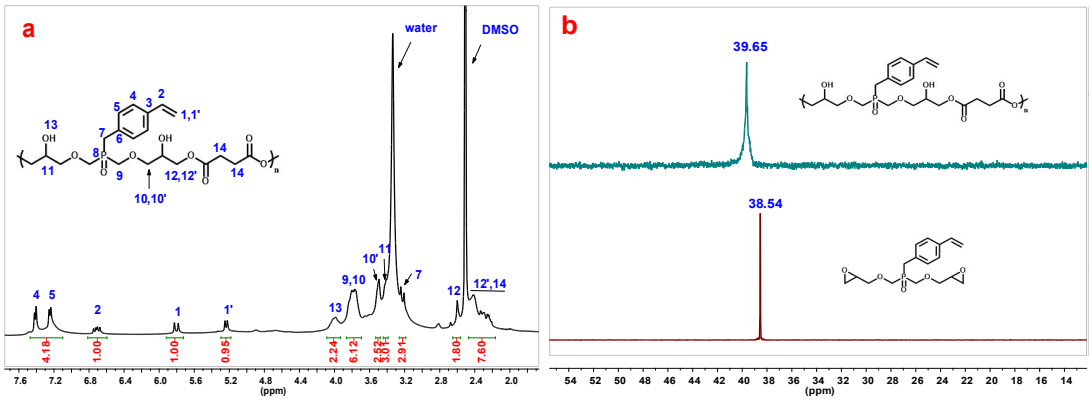

Figure S15. (a) ^{1}H and (b) ^{31}P NMR spectra of P2 in DMSO-d_6.

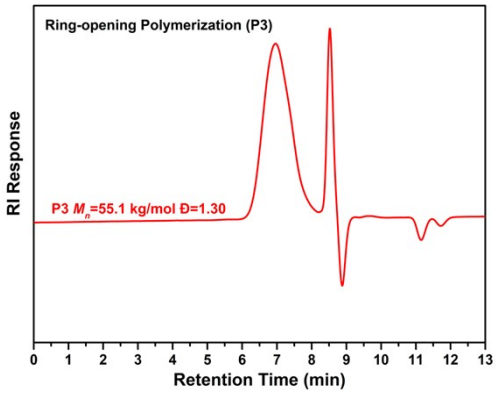

Figure S16. SEC elution curves of poly(β-hydroxyl amine)s (P3).

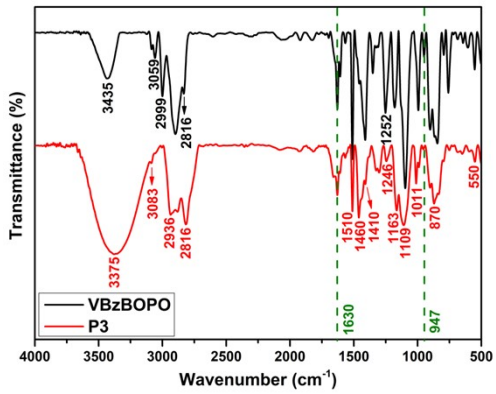

Figure S17. FT-IR spectra of VBzBOPO and P3.

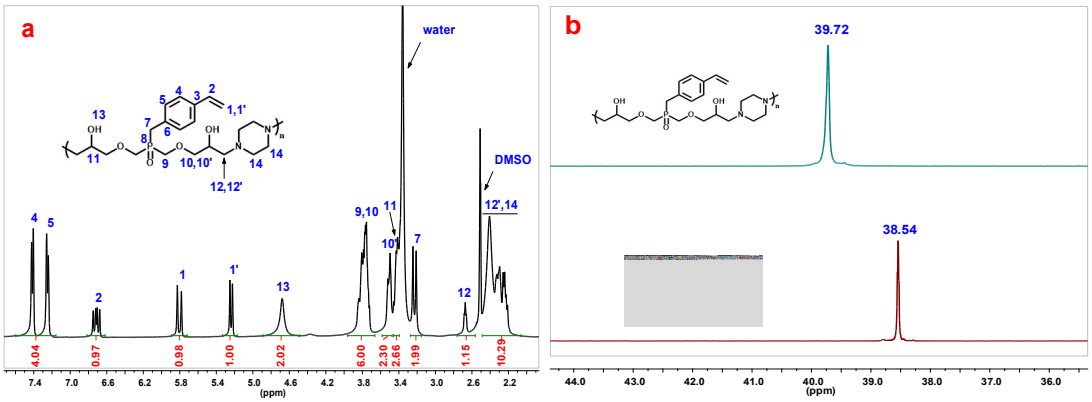

Figure S18. (a) ^{1}H and (b) ^{31}P NMR spectra of P3 in DMSO-d_6.

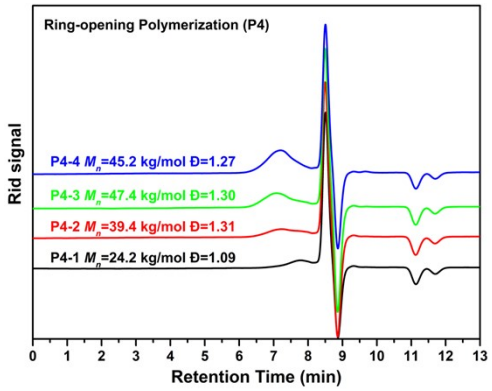

Figure S19. SEC elution curves of poly(β-hydroxythio-ether)s (P4).

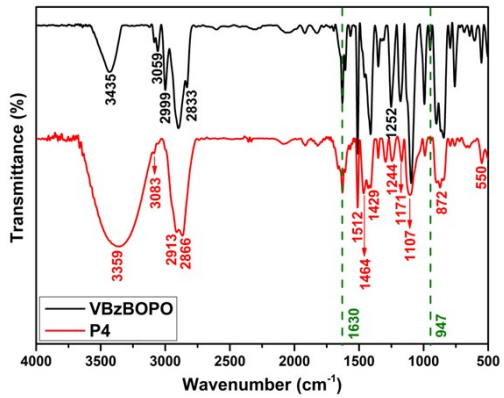

Figure S20. FT-IR spectra of VBzBOPO and P4.

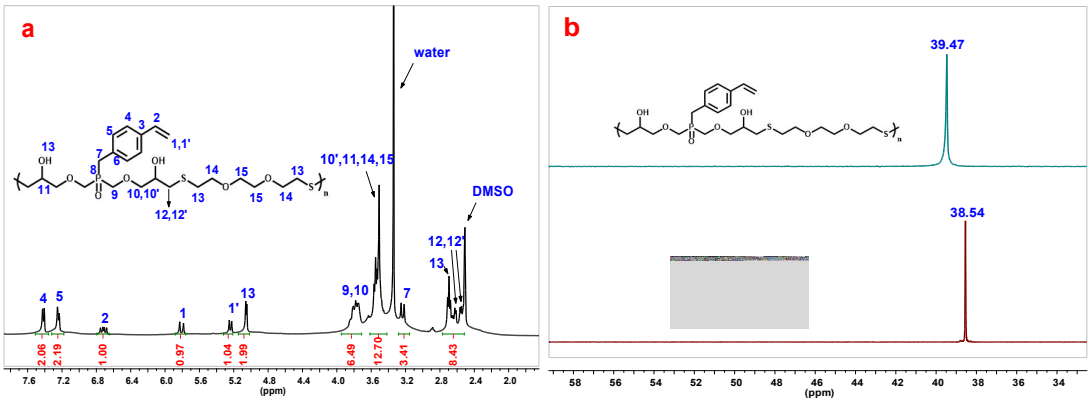

Figure S21. (a) ^{1}H and (b) ^{31}P NMR spectra of P4 in DMSO-d_6.

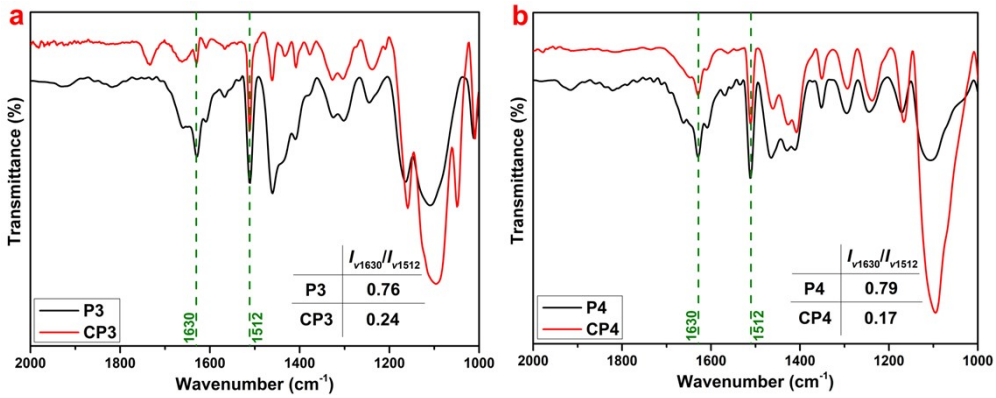

Figure S22. FT-IR spectra of (a) P3 and CP3; (b) P4 and CP4.

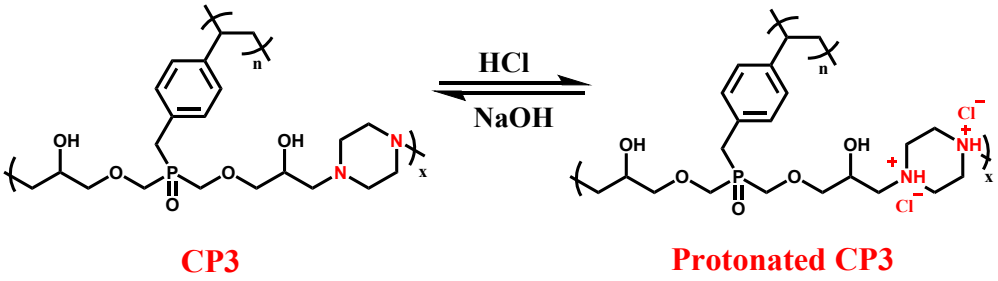

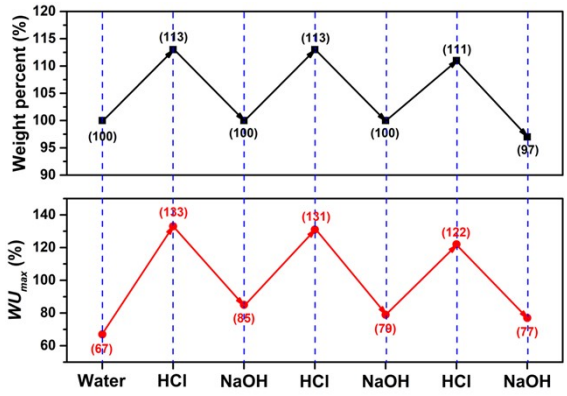

Figure S23. pH-response of CP3 in aqueous HCl or NaOH.

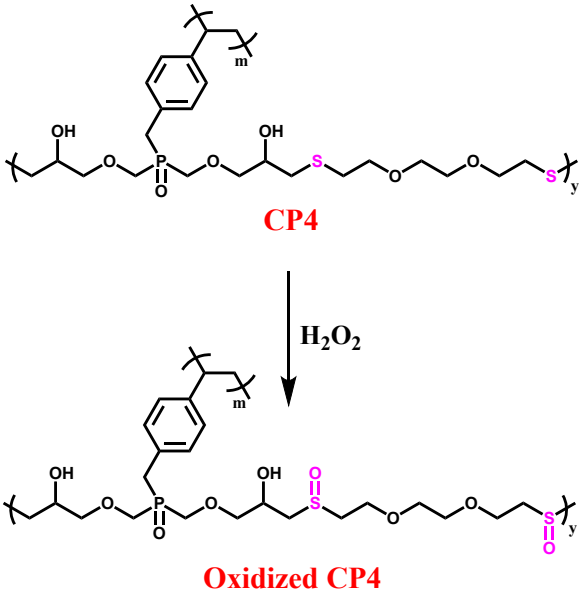

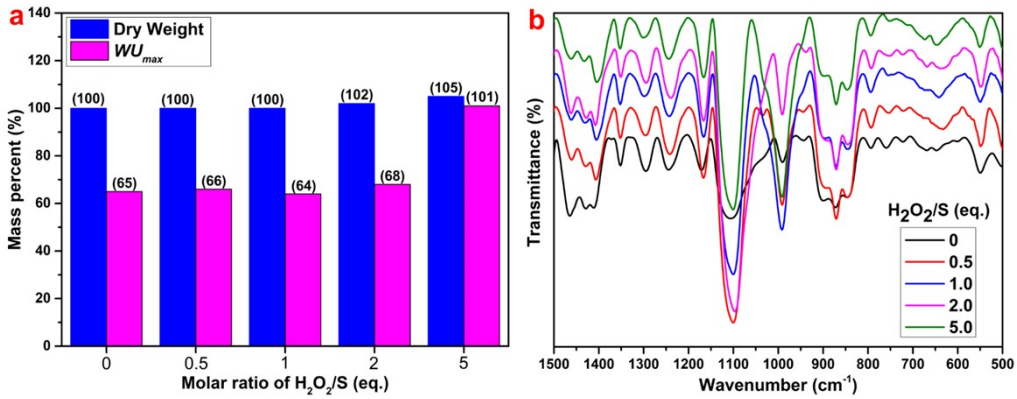

Figure S24. H_2O_2-response of CP4: (a) mass percent and (b) FT-IR spectra.

Table S1. Results of free radical polymerization of VBzBOPO (P1) [a].

P1	Solvent	Initiator (mol%)		*Conv.* (%) [c]	$M_{n,SEC}$ [d] (kg·mol^{-1})	$Đ$ [e]
P1-1	DMAc	BPO	1.0	60	48.1	1.19
P1-2	DMAc	BPO	0.5	69	83.1	1.52
P1-3 [b]	DMAc	AIBN	1.0	57	93.2	1.38
P1-4	DMAc	AIBN	1.0	64	86.4	1.33
P1-5	NMP	BPO	1.0	70	61.4	1.32
P1-6	DMSO	BPO	1.0	27	52.1	1.21
P1-7	DMF	BPO	1.0	50	72.9	1.33

[a] All the experiments was carried out at 90 ℃ for 24 h with 0.8 mol·L^{-1} (ca. 25wt%) of the initial monomer concentration in the organic solvent unless stated otherwise; [b] The polymerization temperature was set as 70 ℃; [c] The monomer conversions were determined by ^{1}H NMR spectra; [d] SEC(DMF) results of polymers; [e] $Đ=M_w/M_n$.

Table S2. RAFT polymerization of VBzBHPO by using AIBN as initiator [a].

time (h)	*Conv.* (%) [b]	$Ln([M]_0/[M])$ [c]	$M_{n,th}$ [d] (kg/mol)	$M_{n,SEC}$ [e] (kg/mol)	$Đ$ [e]
1	17	0.1863	11.8	47.0	1.13
2	34	0.4155	23.3	58.4	1.14
3	40	0.5108	27.3	64.2	1.14
4	55	0.7985	37.5	69.0	1.14
5	60	0.9163	40.9	75.5	1.15
8	70	1.2040	47.6	77.8	1.16
12	86	1.9661	58.5	90.8	1.19
24	97	3.5066	65.9	100.0	1.23

[a] RAFT polymerization condition: $[VBzBOPO]_0$: $[BBTC]_0$: $[AIBN]_0$ =200:1:0.3 at 70 ℃, initial monomer concentration was 40 wt% in DMAc; [b] Determined by ^{1}H NMR spectra; [c] $Ln([M]_0/[M]) = Ln[1/(1-Conv.\%)]$; [d] Calculated by equation 1; [e] Determined by SEC (DMF) and $Đ=M_w/M_n$.

Table S3. RAFT polymerization of VBzBHPO by using BPO as initiator [a].

time (h)	*Conv.* (%) [b]	$Ln([M]_0/[M])$ [c]	$M_{n,th}$ [c] (kg/mol)	$M_{n,SEC}$ [d] (kg/mol)	M_w/M_n [d]
1	30	0.3567	20.6	55.1	1.14
2	37	0.4620	25.3	62.3	1.14
3	47	0.6349	32.1	68.7	1.14
4	53	0.7550	36.1	72.8	1.14
5	57	0.8440	38.8	75.6	1.15
8	60	0.9163	40.9	81.1	1.16
12	62	0.9676	42.2	81.7	1.15
24	69	1.1712	47.0	85.4	1.17

[a] RAFT polymerization condition: $[VBzBOPO]_0$: $[BBTC]_0$: $[BPO]_0$ =200:1:0.3 at 90 °C, initial monomer concentration was 40 wt% in DMAc; [b] Determined by ^1H NMR spectra; [c] $Ln([M]_0/[M]) = Ln[1/(1-Conv.\%)]$; [d] Calculated by equation 1; [e] Determined by SEC (DMF) and $Đ=M_w/M_n$.

Table S4. Ring-opening polycondensation of VBzBOPO with DODT (P4) [a].

P4	Catalyst [b]	Solvent	Temperature / Time (°C/h)	*yield* (%) [c]	$M_{n,SEC}$ [d] (kg·mol^{-1})	$Đ$ [d,e]
P4-1	$LiOH·H_2O$	$DMSO/H_2O$ [f]	r.t./48 h	53	24.2	1.09
P4-2	TEA	DMSO	r.t./48 h	46	39.4	1.31
P4-3	TEA	DMSO	50 °C/24 h	52	47.4	1.30
P4-4	TEA	DMSO	50 °C/48 h	74	45.2	1.27

[a] VBzBOPO (1.02 g, 3.0 mmol) in the selected solvents (1.5 mL); [b] Catalyst: TEA (15 mol% of epoxide); $LiOH·H_2O$ (5 mol% of epoxide); [c] Yields of polyesters were calculated by gravity; [d] SEC (DMF) results of polymers; [e] $Đ=M_w/M_n$; [f] $DMSO/H_2O$ (10/1, v/v) was used as solvent.

Table S5. Self-crosslinked polymers from P2-P4 [a].

gels	*CP2*	*CP3*	CP4
gel content (%) [b]	96	97	95
WU_{max} (%) [c]	65	67	65

[a] Self-crosslinked reactions were carried out at 60 °C under vacuum; [b] gel contents were calculated by gravity before and after Soxhlet extractions; [c] maximum water uptake (WU_{max}) was calculated as $(m_1\text{-}m_0)/m_0$, where m_0 and m_1 means the mass of dry and wet polymers, respectively.